Accepted Manuscript

Synthesis and apoptosis inducing studies of triazole linked 3-benzylidene isatin derivatives

Atulya Nagarsenkar, Lalita Guntuku, Sravanthi Devi Guggilapu, K. Danthi Bai, Gannoju Srinivasulu, V.G.M. Naidu, Bathini Nagendra Babu

PII: S0223-5234(16)30737-1

DOI: 10.1016/j.ejmech.2016.09.009

Reference: EJMECH 8875

To appear in: *European Journal of Medicinal Chemistry*

Received Date: 9 August 2016

Revised Date: 1 September 2016

Accepted Date: 3 September 2016

Please cite this article as: A. Nagarsenkar, L. Guntuku, S.D. Guggilapu, K. Danthi Bai, G. Srinivasulu, V.G.M. Naidu, B.N. Babu, Synthesis and apoptosis inducing studies of triazole linked 3-benzylidene isatin derivatives, *European Journal of Medicinal Chemistry* (2016), doi: 10.1016/j.ejmech.2016.09.009.

Graphical Abstract

Synthesis and apoptosis inducing studies of triazole linked 3-benzylidene isatin derivatives

Atulya Nagarsenkar,[a] Lalita Guntuku,[b] Sravanthi Devi Guggilapu,[a] K. Danthi Bai,[a] Gannoju Srinivasulu,[a] V. G. M. Naidu,[b,*] Bathini Nagendra Babu[a,*]

[a]*Department of Medicinal Chemistry, National Institute of Pharmaceutical Education and Research (NIPER), Hyderabad 500 037, India*

[b]*Pharmacology and Toxicology Division, National Institute of Pharmaceutical Education and Research (NIPER), Hyderabad 500 037, India*

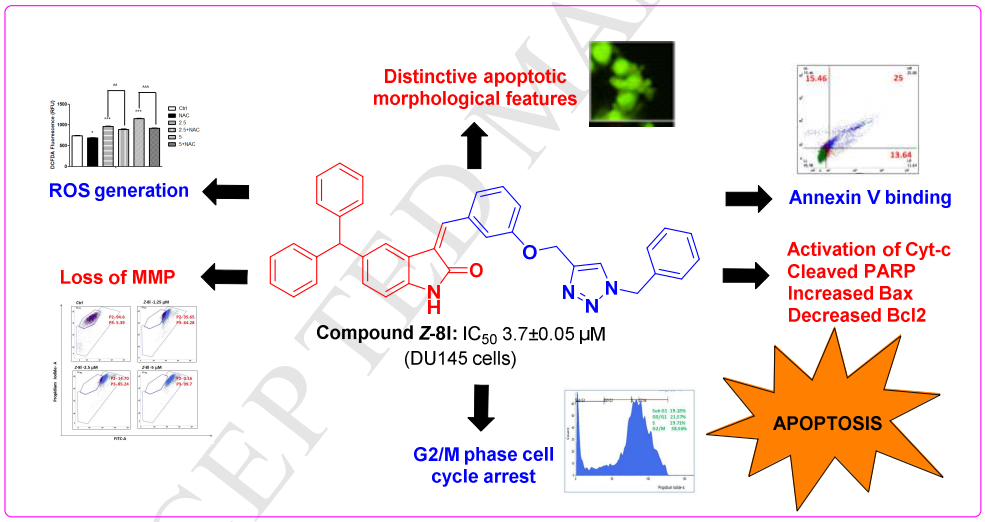

Synthesis and apoptosis inducing studies of triazole linked 3-benzylidene isatin derivatives

Atulya Nagarsenkar,[a] Lalita Guntuku,[b] Sravanthi Devi Guggilapu,[a] K. Danthi Bai,[a] Gannoju Srinivasulu,[a] V. G. M. Naidu,[b,*] Bathini Nagendra Babu[a,*]

[a]*Department of Medicinal Chemistry, National Institute of Pharmaceutical Education and Research (NIPER), Hyderabad 500 037, India*

[b]*Pharmacology and Toxicology Division, National Institute of Pharmaceutical Education and Research (NIPER), Hyderabad 500 037, India*

*Corresponding author:

Dr. Bathini Nagendra Babu
Department of Medicinal Chemistry
National Institute of Pharmaceutical Education and Research
Hyderabad, 500037, India
E-mail: bathini@niperhyd.ac.in; bnniper@gmail.com

Abstract

In our venture towards the development of effective cytotoxic agents, a panel of triazole linked 3-benzylidene isatin hybrids were synthesized and characterized by IR, ^{1}H NMR, ^{13}C NMR and Mass spectral analysis. All the newly synthesized target compounds were assessed against DU145 (prostate), PC-3 (prostate), MDA-MB-231 (breast), BT549 (breast), A549 (lung) and HeLa (cervical) human cancer cell lines by employing MTT assay for their cytotoxic potential. Significantly, compound ***Z*-8l** was found to be most potent amongst all the tested compounds with an IC_{50} value of (3.7±0.05 µM) on DU145 cells. The most active compound (***Z*-8l**) was also tested on RWPE-1 (normal prostate) cells and was found to be safe compared to the DU145 cells. The influence of the cytotoxic compound ***Z*-8l** on the cell cycle distribution was assessed on the DU145 cell line, exhibiting a cell cycle arrest at the G2/M phase. Additionally, treatment with compound ***Z*-8l** caused collapse of mitochondrial membrane potential (DΨm) in DU145 cells. Moreover, acridine orange/ethidium bromide staining, DAPI nuclear staining, DCFDA staining and annexin V binding assay confirmed that compound ***Z*-8l** can induce cell apoptosis in DU145 cells. Western blotting was performed to examine the appearance of active forms of cytochrome c, Bax, Bcl2 and PARP (Poly ADP ribose polymerase), indicator proteins of apoptosis in DU145 cells; the study confirmed the triggering of mitochondrial mediated apoptotic pathway upon exposure of compound ***Z*-8l**.

Keywords: Triazole, oxindole, 3-benzylidene isatin, anticancer, Knoevenagel condensation, apoptosis.

1.0 Introduction

Cancer is one of the foremost global health burden and most severe clinical problems in the world with increasing frequency every year [1]. Regardless of avoiding behavioral risk factors such as tobacco, obesity, and preventive managements like dietary, medication and vaccination, the disease still affects millions of patients worldwide [2]. Many of the current anticancer drugs usually act on rapidly proliferating cells, and may have poor selectivity between normal and cancerous cells. The high toxicity and poor tolerance of the existing anticancer drugs, stress on the need to identify novel molecules with potent antitumor activity, low toxicity and minimum side effects. Thus, the design and synthesis of new chemical entities for the effective and safe cure of cancer is a dynamic area of research in medicinal chemistry.

The oxindole is a privileged scaffold, which represents a vital class of heterocyclic compounds bestowed with interesting pharmacological activities [3] such as inhibitors of the MDM2-p53 interaction [4], cholinesterases [5], antimicrobial [6], histone deacetylases [7], and anticancer properties [8, 9]. In addition, sunitinib and nintedanib (**Figure 1**) are the representative drugs emerged from this class and are in clinical use for targeted anticancer therapies [10]. The FDA approval of sunitinib and nintedanib paved the way to develop various indolin-2-one based molecules against cancer [11, 12].

Principally, the structural modifications at the C3- and C5-positions of the oxindole ring have led to many derivatives possessing increased antitumor activity [1].

<Insert Figure 1 here>

It is well-known that substituted 3-benzylidene isatin scaffold is strongly related with anticancer activity [13]. It has several targets, most of which are directly connected to

oncogenesis [14, 15]. Moreover, Zhang et. al, have proposed that functionalized 3-benzylidene isatins may be included as compounds with chemopreventive potential [15]. The presence of the Michael acceptor motif makes the 3-benzylidene isatin scaffold a probable candidate for such activity. If antitumour 3-benzylidene isatins hold chemopreventive properties, this may mean that when deployed for their effects on cancer cells, the same agent would bestow cytoprotection to normal/non-metastasized cells, a motivating proposition with potential clinical benefits.

On the other hand, the chemistry of 1,2,3-triazoles has received considerable attention due to their synthetic and effective biological importance [16]. Triazole ring is a potential pharmacophore that has been significantly acknowledged over the past few decades [17]. Even though 1,2,3-triazole moiety itself does not occur in nature, there are several examples in literature that show assorted biological activities associated with this system, such as anti-HIV activity [18], antimicrobial activity [19], β3-selective adrenergic agonism [20], kinase inhibitory [21] and other enzyme inhibitory activities [22]. 1,2,3-Triazole moieties have been incorporated into a wide diversity of therapeutically interesting drug candidates; for example (**Figure 1**), antibacterial agents β-lactam (tazobactam), cefatrizine (Trizicef) and anticancer agents (carboxyamidotriazole CAI).

Molecular hybridization is an efficient tool to design more active and new chemical entities by covalently combining two or more drug pharmacophores into a single molecule [23]. Of late, it has been observed that chromone-pyrazole, chromone-pyrimidine, chromone-indolinone, indole-indolinone, indole-pyrimidine and indole-pyrazole conjugates demonstrated profound growth inhibitory activity against different cancer cells [24, 25].

In this context, we desire to exploit 1-benzyl-4-(phenoxymethyl)-1*H*-1,2,3-triazoles as the diversity surrogate to condense with various substituted oxindoles to explore the dual pharmacophoric potential (**Figure 2**). These triazole linked 3-benzylidene isatin hybrids may

have the advantages of tunable anticancer activity and structural diversity. Additionally, the chemical processes and reactions drawn in are facile and concise, which make it feasible for the bulk production of important isatin derivatives.

<Insert Figure 2 here>

2.0 Results and discussion

2.1 Chemistry

The synthesized 3-(3-((1-phenyl-1*H*-1,2,3-triazol-4-yl)methoxy)benzylidene)indolin-2-one **[*E*-8(a-b, d, f-m)** and ***Z*-8(a-c, e, i, k-m)]** compounds of this study comprise two core structural elements: (i) 3-benzylidene isatin, and (ii) a substituted 1,2,3-triazole moiety. Initially, for the preparation of the substituted triazole aldehyde **6** required for the synthesis of proposed target compounds, we have utilized commercially available benzyl bromide **1** as the starting material (**Scheme 1**). The benzyl azide **2(a,b)** was synthesized *via* bimolecular displacement of the halide substituent of benzyl halide **1(a,b)** precursor with an azide nucleophile [26]. Meanwhile, 3-hydroxy benzaldehyde **3** was subjected to *N*-propargylation for the synthesis of respective alkyne **5** [27]. This terminal alkyne bearing substrate **5** was further subjected to [3+2] cycloaddition with benzyl azide **2(a,b)** to afford substituted triazole aldehyde **6(a,b)** [28]. Knoevenagel condensation was employed on oxindole **7a** by using triazole aldehyde **6a** to afford 3-(3-((1-phenyl-1*H*-1,2,3-triazol-4-yl)methoxy)benzylidene)indolin-2-ones in an equal mixture of *E*/*Z* isomeric forms **(*E*-8a+*Z*-8a)** [29]. The reaction was also tried by using dimethoxy triazole aldehyde **6b** to afford consequent final compound. This too was obtained in an equal mixture of *E*/*Z* isomeric forms **(*E*-8b+*Z*-8b)**.

Next, various substituted oxindoles **(7b-g)** were subjected to Knoevenagel condensation by using triazole aldehyde **6a** to get subsequent condensed products. Surprisingly, the target

compounds from 5-Cl **(7b)** and 5-Br **(7d)** oxindoles were obtained as mixture of *E*/*Z* isomeric forms in 20:80 ratios, whereas in case of other oxindoles **(7c, e-g)**, the target compounds were obtained as mixture of *E*/*Z* isomeric forms in 70:30 ratios. Encouraged by such interesting observations, 5-acylated oxindoles **(7h-i)** were used and upon Knoevenagel condensation gave corresponding target compounds. 5-Acetyl oxindole bearing product was obtained in an equal mixture of *E*/*Z* isomeric forms **(*E*-8i+*Z*-8i)**, whereas 5-benzoyl oxindole bearing compound was obtained as *E*/*Z* mixture in 90:10 ratios. Furthermore, 5-alkylated **(7j-l)** oxindoles were subjected to Knoevenagel condensation using triazole aldehyde **6a**. However, the target molecules were obtained in an equal mixture of *E*/*Z* isomeric forms **[*E*-(8k-m)** and **Z-(8k-m)]**. Finally, these *E*/*Z* isomers were separated by using the conventional column chromatography. It has to be noted that in cases where the target compounds were obtained in unequal ratios, we were only able to isolate the major isomer in pure form.

<Insert Scheme 1 here>

The earlier literature reports suggest that the ortho protons (C2'- or C6'-protons) of the benzylidene ring in *Z* isomer are deshielded relative to those in *E* isomer [13, 30]. This deshielding of C2'- or C6'-protons could be due to the presence of nearby C2-position carbonyl of indolin-2-one ring in the *Z* isomer form. So, the two isomer forms can be easily distinguished by ^{1}H NMR analysis.

The stereochemistry was assigned for one of the representative compounds ***Z*-8a** by detailed NOE studies. The ^{1}H and ^{13}C NMR assignments for compound ***Z*-8a** were carried out using gDQFCOSY and ROESY experiments in DMSO-d_6 at 27 °C Bruker 500 MHz (for ^{1}H NMR) and 125 MHz (for ^{13}C NMR), respectively [see ESI†]. The presence of NOE between H5-H6 and H6-H7 in ROESY experiment confirms the geometry at double bond and the compound was characterized as *Z*-isomer as depicted in **Figure 3** and **4**.

<Insert Figure 3 here>

<Insert Figure 4 here>

2.2 Pharmacology

2.2.1 *In vitro* anticancer activity

All synthesized compounds were evaluated for their *in vitro* cytotoxic activity against six human cancer cell lines DU145 (prostate), PC-3 (prostate), MDA-MB-231 (breast), BT549 (breast), A549 (lung) and HeLa (cervical) cancer cell lines by employing MTT assay [31]. Sunitinib was taken as the reference in this study. Concentration response course analysis was executed to determine drug concentrations required to inhibit the growth of cancer cells by 50% (IC_{50}) after incubation for 48 h. The results of *in vitro* anticancer activity revealed that, some of the synthesized compounds exhibited different levels of anticancer properties (**Table 1**).

From the close analysis of the IC_{50} values, it was observed that, that the Knoevenagel product **(*Z*-8a)** of oxindole and aldehyde **(6a)** was moderately active only against PC-3 and A549 cell lines, while its *E* isomer **(*E*-8a)** was found to be active against DU145, PC-3 and HeLa. Target compound **(*Z*-8b)** synthesized using dimethoxy substituted aldehyde **(6b)** showed moderate activity against PC-3, A549 and HeLa; whereas its *E* isomer **(*E*-8b)** displayed remarkable activity against MDA-MB-231 cells along with moderate activity towards other tested cell lines.

Target compounds with 5-chloro **(*Z*-8c)**, 6-chloro **(*E*-8d)** and 5-bromo **(*Z*-8e)** substitutions on oxindole were specifically active against DU145, whereas compound with 6-bromo **(*E*-8f)** substitution displayed significant activity towards DU145 and A549 cell lines. The compounds with 5-fluro **(*E*-8g)** and 5-nitro **(*E*-8h)** substitutions on oxindole were found to be inactive towards all the tested cell lines. Compound bearing 5-acetyl **(*Z*-8i)** substitution on

oxindole exhibited moderate activity selectively against A549, whereas its *E* isomer **(*E*-8i)** was inactive. Compound containing 5-benzoyl **(*E*-8j)** substitution was inactive towards all tested cell lines.

The target molecule with 5-*p*-methoxy benzyl substitution on oxindole **(*Z*-8k)** displayed striking activity towards DU145 and HeLa cell lines; on the other side its *E* isomer **(*E*-8k)** was moderately active against PC-3. Target compound holding bulky benzhydryl substitution at 5^{th} position of oxindole **(*Z*-8l)** demonstrated remarkable activity against all the tested cell lines except MDA-MB-231 cells. However, its *E* isomer **(*E*-8l)** was found to be inactive towards all tested cell lines. The compound having *p*-methyl substitution on diphenyl propargyl moiety **(*Z*-8m)** was found to be inactive against all the tested cell lines, though its *E* isomer **(*E*-8m)** showed moderate activity against DU145, A549 and HeLa.

The most active compound **(*Z*-8l)** was also tested on normal prostate (RWPE-1) cells and was found to be safe compared to the DU145 prostate cancer cells. Additionally, aldehyde **(6a)** was screened for its anticancer potential and was found to be inactive against all tested cell lines.

Analysis of the MTT assay results suggests DU145 cells are more sensitive towards the synthesized target compounds. The impact of modification of the "R_1" group on 5^{th} position of oxindole derivatives is interesting in the light of the results of the SAR study, which suggests that bulky aryl groups at 5^{rd} position of oxindole is optimal for anticancer activity. However, it has to be noted that *Z* isomers of 5-*p*-methoxy benzyl and 5-benzhydryl substituted oxindole compounds showed better results than its *E* isomers. On the other hand simple halogen substitutions at this position demonstrated increase in selectivity towards DU145 cell lines. Further derivatization has mostly resulted in a significant loss of activity. Among all compounds synthesized, compound **(*Z*-8l)** showed the most significant cytotoxicity towards most of the tested cancer cell lines. These primary results persuade

further assessment on the synthesized compounds aiming to the development of novel potential anticancer agents.

<Insert Table 1 here>

2.2.2 Acridine orange–ethidium bromide (AO–EB) staining

Acridine orange/ethidium bromide (AO/EB) fluorescent staining assay was performed to distinguish the live, apoptotic and necrotic cells [32]. AO permeates the intact cell membrane and stains the nuclei green, while EB can stain the cells that have lost their membrane integrity and tinge the nucleus red. It can be interpreted from **Figure 5** that the control cells showed the normal healthy morphology with intact nuclear architecture and appeared green in colour. Fluorescence microscopic images of ***Z*-8l** treated DU145 cells have clearly demonstrated morphological changes which are the characteristic features of apoptotic cells such as cell shrinkage, membrane blebbing and apoptotic body formation. This confirms that the compound ***Z*-8l** induced cell death in DU145 cancer cells.

<Insert Figure 5 here>

2.2.3 DAPI Nucleic Acid Staining

DAPI (4',6-diamidino-2-phenylindole) is a fluorescent dye that binds sturdily to nucleus and detect the nuclear damage or chromatin condensation. The DAPI stains the apoptotic cells as bright colored owing to the condensed nucleus which is a distinctive apoptotic characteristic. Hence, it was of our interest to detect nuclear damage or chromatin condensation persuaded by the compound ***Z*-8l** in DU145 cells. DAPI staining technique was performed according to the earlier reported method [33]. The results from the **Figure 6** illustrated that the nuclear structure of untreated cells was intact whereas compound ***Z*-8l** treated cells exhibited condensed, pyknotic, or fragmented nuclei.

<Insert Figure 6 here>

2.2.4 Cell cycle analysis

Many of the cytotoxic compounds exert their growth inhibitory effect by arresting the cell cycle at a specific phase of a cell cycle. *In vitro* screening results revealed that the compound ***Z*-8l** showed significant activity against DU145 cells. Thus, we herein examined the effect of the compound ***Z*-8l** on cell cycle using propidium iodide staining method [34].

DU145 cells were treated with designated concentrations of compound **Z-8l** for 24 h. They were stained with propidium iodide and samples were further analysed by flow cytometry. Treatment with the compound ***Z*-8l** at 2.5 and 5 µM in DU145 cells displayed rise in G2/M population from 29.66% (control) to 43.74% and 48.02% respectively in a dose dependent manner (**Figure 7**). The results suggest clear induction of G2/M cell cycle arrest by the test compound. Furthermore, increase in sub G1 population compared to control also indicates the induction of apoptotic death in the treated cells.

<Insert Figure 7 here>

2.2.5 Annexin V binding assay

The apoptosis inducing effect of compound ***Z*-8l** on DU145 cancer cells was further investigated using annexin V-FITC/propidium iodide staining assay [35]. DU145 cells were treated with 1.25, 2.5 and 5 µM of compound ***Z*-8l** for 24 h and stained with Annexin V-FITC and propidium iodide, and samples were analysed by flow cytometry.

As depicted in **Figure 8**, ***Z*-8l** treated DU145 cells demonstrated rise in the total percentage of apoptotic (early and late apoptotic cells- Annexin V +ve cells) and dead cells from 9.68% (untreated) to 23.53%, 35.46% and 54.1% respectively in a dose dependent manner.

<Insert Figure 8 here>

2.2.6 Measurement of reactive oxygen species (ROS) levels

The reactive oxygen species generation is one of well characterised mechanisms of many anticancer drugs. Hence, in next array of experiments, we assessed the generation of intracellular reactive oxygen species by compound ***Z*-8l** in DU145 cells using DCFDA staining method [36].

Treatment with compound ***Z*-8l** for 6 h resulted in significant increase in DCFDA fluorescence in a dose dependent manner, signifying ROS accumulating property of compounds (**Figure 9**). Treatment with *N*-acetyl cysteine (NAC) prior to compound treatment has decreased DCFDA fluorescence intensity; this indicated that compounds induced cytotoxicity by ROS generation.

<Insert Figure 9 here>

2.2.7 Analysis of Mitochondrial Membrane Potential (DΨm)

Increase in intracellular ROS can cause oxidative stress and lead to the loss of mitochondrial membrane potential. Thus, the effect of compound ***Z*-8l** on mitochondrial membrane potential (DΨm) was determined by staining with lipophilic cationic JC-1 dye [37]. Healthy polarised mitochondria stains red due to potential dependent formation of J-aggregates, while depolarised mitochondria in apoptotic cells stains green because of J-monomers DU145 cells were treated with 1.25, 2.5 and 5 μM of ***Z*-8l** for 24 h and stained by JC-1 dye . Flowcytometric analysis of the treated cells clearly displayed increase in depolarised cell population (P2) from control (5.39%) to 64.28%, 85.24% and 99.7% respectively in conc. dependent manner (**Figure 10**). Thus, the results clearly indicate loss of mitochondrial membrane potential by the compound ***Z*-8l** and suggest the involvement of mitochondria dependent apoptotic pathway in their mechanism of action.

<Insert Figure 10 here>

2.2.8 Western blotting analysis

Cytochrome c, Bax, Bcl2 and PARP are some of the proteins whose expression plays a critical role in the apoptotic process. Particularly, PARP (Poly ADP ribose polymerase) is 116 kda protein that gets cleaved into 89 kda protein fragment during caspases activation and this cleavage is prominent hallmark of the apoptosis induction. Intrinsic or mitochondria mediated apoptotic pathway can be evidenced with loss of mitochondrial membrane potential usually preceded by the release of cytochrome c into cytosol. Herein, to investigate the molecular mechanisms of compound ***Z*-8l** on apoptosis, we have checked the expression of Bcl2, Bax, PARP and cytochrome c by using western blot method [38]. Results from the **Figure 11** indicated that compound ***Z*-8l** treatment led to the dose dependent increased expression of cleaved PARP and cytochrome c in DU145 cells, which is a hallmark feature of apoptosis. Moreover, the compound ***Z*-8l** treatment resulted in decreased expression of anti-apoptotic Bcl2 and increased expression of proapoptotic Bax proteins in a dose dependent manner. Collectively, these results illustrate that compound ***Z*-8l** induced apoptosis through apoptosis-related protein expression.

<Insert Figure 11 here>

3.0 Conclusion

In the current study, novel triazole linked benzylidene-isatin derivatives were synthesized, and were further evaluated for their *in vitro* anticancer potentials. An initial screening was performed against DU145, PC-3, MDA-MB-231, BT549, A549 and HeLa human cancer cell lines. In MTT assay, the compound ***Z*-8l** was found to be the most active against the DU145 (prostate cancer) cell line. Most importantly, the compound ***Z*-8l** was found to be

comparatively safe towards normal cell line RWPE-1. The detailed studies like AO/EB staining and Annexin V binding assay and DAPI nuclear staining suggested that compound ***Z*-8l** induced apoptosis in DU145 cells. The cell cycle analysis confirmed that the compound ***Z*-8l** target the G2/M phase of DU145 cell cycle in a dose-dependent manner. Moreover, the compound ***Z*-8l** treatment resulted in collapse of mitochondrial membrane potential and elevated intracellular ROS levels in DU145 cells. Investigation of expression levels of apoptotic proteins cytochrome c, Bax, Bcl2 and cleaved PARP in DU145 cells revealed that compound ***Z*-8l** trigger mitochondrial mediated intrinsic pathway thereby inducing apoptosis in cancer cells. Overall, the current studies demonstrated that dual pharmacophores strategy can be useful in the synthesis of promising new chemical entities for the development of cancer therapeutics.

4.0 Experimental protocols

4.1 Chemistry

All reagents and solvents were obtained from commercial suppliers and were used without further purification. Analytical thin layer chromatography (TLC) was performed on MERCK precoated silica gel 60-F-254 (0.5 mm) aluminium plates. Visualization of the spots on TLC plates was achieved UV light. ^{1}H and ^{13}C NMR spectra were recorded on bruker 500 MHz spectrometer using tetramethyl silane (TMS) as the internal standard. Chemical shifts for ^{1}H and ^{13}C are reported in parts per million (ppm) downfield from tetramethyl silane. Spin multiplicities are described as s (singlet), bs (broad singlet), d (doublet), dd (double douplet), t (triplet), q (quartet), and m (multiplet). Coupling constant (*J*) values are reported in hertz (Hz). IR spectra were recorded on a Perkin Elmer, FT-IR spectrometer using KBr discs. HRMS were determined with Agilent QTOF mass spectrometer 6540 series instrument. Column chromatography was performed using silica gel 60-120.

4.2 General procedure for the synthesis of 3-(prop-2-yn-1-yloxy)benzaldehyde (5)

To a stirred solution of 3-hydroxy benzaldehyde **3** (1 equiv.) in acetonitrile was added propargyl bromide **4** and potassium carbonate (5 equiv.) and refluxed for 6 h. Completion of the reaction was checked by TLC (*n*-hexane/EtOAc; 7:3). Solvent was evaporated under reduced pressure. Compound was extracted using ethyl acetate and water. Organic layer was separated and concentrated. The compound was purified using column chromatography (*n*-hexane/ethyl acetate) to give pure compound **5** in good yield.

4.3 General procedure for the synthesis of substituted triazole aldehyde 6(a,b)

To a stirred solution of 3-(prop-2-yn-1-yloxy)benzaldehyde **5** (1 equiv.) in *t*-butanol/water (1:1) was added CuI (0.01 equiv.) and azide **2** (1 equiv.) and heated at 40 °C for 48 h. Completion of the reaction was checked by TLC (*n*-hexane/EtOAc; 5:5). Solvent was evaporated under reduced pressure. Compound was extracted using ethyl acetate and water. Organic layer was separated and concentrated. The compound was purified using column chromatography (*n*-hexane/ethyl acetate) to give pure compound **6(a,b)** in good yields.

4.4 General procedure for the synthesis of triazole linked benzylidene-isatin derivatives [*E*-8(a-b, d, f-m) and *Z*-8(a-c, e, i, k-m)]

To a stirred solution of oxindole **7** (1 equiv) in ethanol was added substituted triazole aldehyde **6** (1 equiv) and piperidine (0.01 equiv) and refluxed for 3 h. Completion of the reaction was checked by TLC (*n*-hexane/EtOAc; 3:7). The product was filtered and was purified using column chromatography (*n*-hexane/ethyl acetate) to give pure compound **[*E*-8(a-b, d, f-m)** and ***Z*-8(a-c, e, i, k-m)]** in good yields.

4.4.1 (*Z*)-3-(3-((1-Benzyl-1*H*-1,2,3-triazol-4-yl)methoxy)benzylidene)indolin-2-one (*Z*-8a)

Yellow solid; yield: 45%; mp 198-200 °C. IR (KBr): 3320, 2781, 1705, 1610, 1453, 1075, 788 cm^{-1}. ^1H NMR (500 MHz, DMSO-d_6): δ = 10.60 (s, 1H), 8.33 (t, *J* = 2.0 Hz, 1H), 8.29 (s, 1H), 7.82 (d, *J* = 7.6 Hz, 1H), 7.77 (s, 1H), 7.69 (d, *J* = 7.6 Hz, 1H), 7.36-7.28 (m, 6H), 7.21 (t, *J* = 7.6 Hz, 1H), 7.11 (dd, *J* = 8.0 2.0, Hz, 1H), 6.98 (t, *J* = 7.6 Hz, 1H), 6.82 (d, *J* = 7.6 Hz, 1H), 5.60 (s, 2H), 5.18 (s, 2H) ppm. ^{13}C NMR (125 MHz, DMSO-d_6): δ = 166.9, 157.5, 142.7, 140.6, 136.5, 135.8, 135.1, 129.1, 128.9, 128.6, 128.0, 127.8, 126.9, 125.1, 124.7, 124.6, 121.0, 119.7, 117.2, 117.0, 109.2, 61.0, 52.7 ppm. HRMS (ESI): *m/z* calcd. for $C_{25}H_{20}N_4O_2$ $[M+H]^+$ 409.1665; found 409.1663.

4.4.2 (*E*)-3-(3-((1-Benzyl-1*H*-1,2,3-triazol-4-yl)methoxy)benzylidene)indolin-2-one (*E*-8a)

Yellow solid**;** yield: 39%; mp 185-189 °C. IR (KBr): 3318, 2793, 1703, 1604, 1445, 1058, 811 cm^{-1}. ^1H NMR (500 MHz, DMSO-d_6): δ = 10.59 (s, 1H), 8.29 (s, 1H), 7.59 (s, 1H), 7.52 (d, *J* = 7.7 Hz, 1H), 7.44 (t, *J* = 7.7 Hz, 1H), 7.36 (d, *J* = 7.2 Hz, 2H), 7.34-7.29 (m, 5H), 7.25 (t, *J* = 7.6 Hz, 2H), 7.14 (d, *J* = 8.2 Hz, 1H), 6.89-6.82(m, 1H), 5.62 (s, 2H), 5.20 (s, 2H) ppm. ^{13}C NMR (125 MHz, DMSO-d_6): δ = 168.4, 158.0, 142.8, 142.7, 135.8, 135.7, 135.4, 130.0, 129.8, 128.6, 128.0, 127.8, 127.7, 124.6, 122.4, 121.6, 121.0, 120.7, 116.2, 115.1, 110.0, 61.1, 52.7 ppm. HRMS (ESI): *m/z* calcd. for $C_{25}H_{20}N_4O_2$ $[M+H]^+$ 409.1665; found 409.1691.

4.4.3 (*Z*)-3-(3-((1-(3,5-Dimethoxybenzyl)-1*H*-1,2,3-triazol-4-yl)methoxy)benzylidene) indolin-2-one (*Z*-8b)

Yellow solid; yield: 31%; mp 223-225 °C. IR (KBr): 3298, 2883, 1706, 1610, 1448, 1212, 1068, 813 cm^{-1}. ^1H NMR (500 MHz, DMSO-d_6): δ = 10.62 (s, 1H), 8.34 (s, 1H), 8.31 (s, 1H), 7.84 (d, *J* = 7.7 Hz, 1H), 7.77 (s, 1H), 7.70 (d, *J* = 7.6 Hz, 1H), 7.41 (t, *J* = 7.9 Hz, 1H), 7.25 (t, *J* = 7.7 Hz, 1H), 7.14 (dd, *J* = 2.1, 8.0 Hz, 1H), 7.02 (t, *J* = 7.7 Hz, 1H), 6.84 (d, *J* = 7.7 Hz, 1H), 6.48-6.43 (m, 3H), 5.52 (s, 2H), 5.19 (s, 2H), 3.70 (s, 6H) ppm. ^{13}C NMR (125

MHz, DMSO-d_6): δ = 166.9, 160.5, 157.5, 142.7, 140.6, 137.9, 136.5, 135.1, 129.1, 128.9, 126.9, 125.1, 124.7, 124.7, 121.0, 119.7, 117.2, 117.0, 109.2, 105.9, 99.5, 60.9, 55.1, 52.7 ppm. HRMS (ESI): *m/z* calcd. for $C_{27}H_{25}N_4O_4$ $[M+H]^+$ 469.1876; found 469.1892.

4.4.4 (*E*)-3-(3-((1-(3,5-Dimethoxybenzyl)-1*H*-1,2,3-triazol-4-yl)methoxy)benzylidene) indolin-2-one (*E*-8b)

Yellow solid; yield: 36%; mp 211-213 °C. IR (KBr): 3356, 3065, 2923, 1703, 1690, 1587, 1456, 1219, 1076, 696 cm^{-1}. ^1H NMR (500 MHz, DMSO-d_6): δ = 10.60 (s, 1H), 8.29 (s, 1H), 7.58 (s, 1H), 7.52 (d, *J* = 7.7 Hz, 1H), 7.46 (t, *J* = 7.9 Hz, 1H), 7.34-7.28 (m, 2H), 7.24 (t, *J* = 7.6 Hz, 1H), 7.15-7.12 (m, 1H), 6.88-6.81 (m, 2H), 6.49-6.44 (m, 3H), 5.52 (s, 2H), 5.19 (s, 2H), 3.70 (s, 6H) ppm.^{13}C NMR (125 MHz, DMSO-d_6): δ = 160.5, 158.0, 142.8, 142.7, 137.9, 136.5, 135.7, 135.4, 130.1, 129.8, 127.7, 124.7, 122.4, 121.6, 121.0, 120.7, 116.2, 115.1, 110.0, 105.9, 99.5, 61.0, 55.1, 52.7 ppm. HRMS (ESI): *m/z* calcd. for $C_{27}H_{25}N_4O_4$ $[M+H]^+$ 469.1876; found 469.1879.

4.4.5 (*Z*)-3-(3-((1-Benzyl-1*H*-1,2,3-triazol-4-yl)methoxy)benzylidene)-5-chloroindolin-2-one (*Z*-8c)

Yellow solid; yield: 60%; mp 198-202 °C. IR (KBr): 3338, 2884, 1704, 1610, 1462, 1462, 1218, 1028, 741 cm^{-1}. ^1H NMR (500 MHz, DMSO-d_6): δ = 10.74 (s, 1H), 8.36 (s, 1H), 8.30 (d, *J* = 3.5 Hz, 1H), 7.91 (s, 1H), 7.85 (m, 1H), 7.66 (s, 1H), 7.50-7.23 (m, 6H), 7.18-7.13 (m, 1H), 6.89 (d, *J* = 8.3Hz, 1H), 6.84 (d, *J* = 8.3Hz, 1H), 5.61 (s, 2H), 5.20 (s, 2H) ppm. ^{13}C NMR (125 MHz, DMSO-d_6): δ = 170.2, 158.1, 157.5, 142.6, 141.6, 137.3, 135.8, 129.9, 129.5, 128.6, 128.0, 127.8, 125.4, 125.3, 124.6, 121.9, 121.5, 116.6, 115.1, 111.4, 110.6, 59.6, 52.7 ppm. HRMS (ESI): *m/z* calcd. for $C_{25}H_{19}ClN_4O_2$ $[M+H]^+$ 443.1275; found 443.1295.

4.4.6 (*E*)-3-(3-((1-Benzyl-1*H*-1,2,3-triazol-4-yl)methoxy)benzylidene)-6-chloroindolin-2-one (*E*-8d)

Yellow solid; yield: 57%; mp 198-202 °C. IR (KBr): 3210, 3064, 2923, 1704, 1690, 1455, 1219, 1054, 696 cm^{-1}. ^1H NMR (500 MHz, DMSO-d_6): δ = 10.77 (s, 1H), 8.30 (m, 1H), 7.63 (s, 1H), 7.52 (d, J = 8.2 Hz, 1H), 7.47 (t, J = 7.9 Hz, 1H), 7.40-7.26 (m, 6H), 7.16 (dd, J = 2.1, 8.0 Hz, 1H), 6.93-6.87 (m, 2H), 5.61 (s, 2H), 5.19 (s, 2H) ppm. ^{13}C NMR (125 MHz, DMSO-d_6): δ = 168.4, 158.0, 144.2, 142.7, 136.3, 135.9, 13.40, 129.9, 129.2, 128.6, 128.0, 127.8, 126.6, 124.6, 123.7, 121.7, 120.9, 119.6, 116.6, 115.1, 110.0, 61.1, 52.7 ppm. HRMS (ESI): *m/z* calcd. for $C_{25}H_{19}ClN_4O_2$ $[M+H]^+$ 443.1275; found 443.1277.

4.4.7 (*Z*)-3-(3-((1-Benzyl-1*H*-1,2,3-triazol-4-yl)methoxy)benzylidene)-5-bromoindolin-2-one (*Z*-8e)

Yellow solid; yield: 63%; mp 201-203 °C. IR (KBr): 3351, 2924, 1703, 1580, 1462, 1253, 1218, 1028, 696 cm^{-1}. ^1H NMR (500 MHz, DMSO-d_6): δ = 10.76 (s, 1H), 8.36 (s, 1H), 8.31 (s, 1H), 7.98-7.95 (m, 1H), 7.92 (s, 1H), 7.86 (d, J = 7.7 Hz, 1H), 7.42-7.29 (m, 7H), 7.17 (dd, J = 1.8, 7.7 Hz, 1H), 6.80 (d, J = 8.2 Hz, 1H), 5.62 (s, 2H), 5.19 (s, 2H) ppm. ^{13}C NMR (125 MHz, DMSO-d_6): δ = 168.7, 158.2, 148.5, 142.6, 141.5, 139.1, 135.9, 134.9, 130.1, 128.7, 128.0, 127.8, 126.5, 124.7, 122.0, 121.1, 117.6, 117.4, 115.0, 110.1, 109.3, 61.2, 52.7 ppm. HRMS (ESI): *m/z* calcd. for $C_{25}H_{19}BrN_4O_2$ $[M+H]^+$ 487.0771; found 487.0773.

4.4.8 (*E*)-3-(3-((1-Benzyl-1*H*-1,2,3-triazol-4-yl)methoxy)benzylidene)-6-bromoindolin-2-one (*E*-8f)

Yellow solid; yield: 55%; mp 196-199 °C. IR (KBr): 3310, 2870, 1704, 1604, 1445, 1240, 1057, 693 cm^{-1}. ^1H NMR (500 MHz, DMSO-d_6): δ = 10.76 (s, 1H), 8.29 (s, 1H), 7.65 (s, 1H), 7.44 (t, J = 8.0 Hz, 2H), 7.38-7.27 (m, 7H), 7.15 (dd, J = 2.2, 8.0 Hz, 1H), 7.06 (dd, J = 1.8, 8.2 Hz, 1H), 7.02 (d, J = 1.8 Hz, 1H), 5.62 (s, 2H), 5.19 (s, 2H) ppm. ^{13}C NMR (125 MHz, DMSO-d_6): δ = 168.2, 158.0, 142.2, 142.7, 136.5, 135.8, 135.4, 129.9, 128.6, 128.0,

127.8, 126.7, 124.6, 123.9, 123.7, 122.5, 121.6, 120.0, 116.6, 115.0, 112.7, 61.1, 52.7 ppm. HRMS (ESI): *m/z* calcd. for $C_{25}H_{19}BrN_4O_2$ $[M+H]^+$ 487.0771; found 487.0763.

4.4.9 (*E*)-3-(3-((1-Benzyl-1*H*-1,2,3-triazol-4-yl)methoxy)benzylidene)-5-fluoroindolin-2-one (*E*-8g)

Yellow solid; yield: 62%; mp 188-190 °C. IR (KBr): 3296, 2919, 1694, 1594, 1469, 1209, 1155, 784 cm^{-1}. ^1H NMR (500 MHz, DMSO-d_6): δ = 10.65 (s, 1H), 8.30 (s, 1H), 7.67 (s, 1H), 7.47 (t, *J* = 7.8 Hz, 1H), 7.40-7.26 (m, 7H), 7.21 (d, *J* = 9.2 Hz, 1H), 7.16 (d, *J* = 8.2 Hz, 1H), 7.12-7.06 (m, 1H), 6.90-6.85 (m, 1H), 5.61 (s, 2H), 5.19 (s, 2H) ppm. ^{13}C NMR (125 MHz, DMSO-d_6): δ = 168.5, 158.1, 142.7, 139.2, 137.2, 135.9, 135.3, 134.9, 130.0, 129.3, 128.7, 128.1, 127.9, 125.4, 124.7, 121.5, 117.5, 117.4, 116.5, 116.4, 115.3, 110.9, 110.8, 61.1, 52.8 ppm. HRMS (ESI): *m/z* calcd. for $C_{25}H_{19}FN_4O_2$ $[M+H]^+$ 427.1574; found 427.1569.

4.4.10 (*E*)-3-(3-((1-Benzyl-1*H*-1,2,3-triazol-4-yl)methoxy)benzylidene)-5-nitroindolin-2-one (*E*-8h)

Yellow solid; yield: 59%; mp 189-191 °C. IR (KBr): 3300, 2870, 1704, 1604, 1444, 1209, 693 cm^{-1}. ^1H NMR (500 MHz, DMSO-d_6): δ = 11.37 (s, 1H), 8.44-8.27 (m, 2H), 8.24-8.14 (m, 2H), 7.52-7.27 (m, 7H), 7.24 (t, *J* = 6.5 Hz, 1H), 7.10 (d, *J* = 8.5 Hz, 1H), 7.04 (d, *J* = 8.2 Hz, 1H), 5.62 (s, 2H), 5.21 (s, 2H) ppm. ^{13}C NMR (125 MHz, DMSO-d_6): δ = 168.7, 158.2, 148.5, 142.6, 141.5, 139.1, 135.9, 130.1, 129.3, 128.7, 128.0, 127.8, 126.5, 124.7, 122.0, 121.1, 117.6, 117.4, 115.0, 110.1, 109.3 ppm. HRMS (ESI): *m/z* calcd. for $C_{25}H_{19}N_5O_4$ $[M+H]^+$ 454.1515; found 454.1513.

4.4.11 (*Z*)-5-Acetyl-3-(3-((1-benzyl-1*H*-1,2,3-triazol-4-yl)methoxy)benzylidene)indolin-2-one (*Z*-8i)

Yellow solid; yield: 30%; mp 210-212 °C. IR (KBr): 3320, 2902, 1693, 1583, 1512, 1241, 1207, 1034, 809 cm^{-1}. ^1H NMR (500 MHz, DMSO-d_6): δ = 10.62 (s, 1H), 8.35 (s, 1H), 8.31

(s, 1H), 7.84 (d, *J* = 7.6 Hz, 1H), 7.77 (s, 1H), 7.70 (d, *J* =7.4 Hz, 1H), 7.39-7.35 (m, 2H), 7.33-7.30 (m, 3H), 7.24 (dt, *J* = 0.9, 7.6 Hz, 1H), 7.14 (dd, *J* = 2.1, 7.9 Hz, 1H), 7.01 (dt, *J* = 0.7, 7.6 Hz, 1H), 6.84 (d, *J* =7.6 Hz, 1H), 5.61 (s, 2H), 5.19 (s, 2H), 2.52 (s, 3H) ppm. ^{13}C NMR (125 MHz, DMSO-d_6): δ = 198.7, 166.7, 157.3, 142.5, 140.4, 136.2, 135.6, 134.8, 128.8, 128.7, 128.4, 127.7, 127.5, 126.6, 124.8, 124.5, 124.4, 120.7, 119.4, 116.9, 116.8, 109.0, 60.7, 52.4, 28.4 ppm. HRMS (ESI): *m/z* calcd. for $C_{27}H_{22}N_4O_3$ $[M+H]^+$ 451.1770; found 451.1772.

4.4.12 (*E*)-5-Acetyl-3-(3-((1-benzyl-1*H*-1,2,3-triazol-4-yl)methoxy)benzylidene)indolin-2-one (*E*-8i)

Yellow solid; yield: 42%; mp 178-180 °C. IR (KBr): 3323, 2989, 1704, 1613, 1588, 1221, 1054, 713 cm^{-1}. ^{1}H NMR (500 MHz, DMSO-d_6): δ = 10.64 (d, *J* = 10.5 Hz, 1H), 8.32 (d, *J* = 7.4 Hz, 1H), 7.59 (s, 1H), 7.46-7.28 (m, 7H), 7.24 (td, *J* = 1.0, 7.5 Hz, 1H), 7.15-7.11 (m, 1H), 7.01-6.97 (m, 1H), 6.88-6.81 (m, 2H), 5.63 (d, *J* = 5.0 Hz, 2H), 5.19 (s, 2H), 2.53 (s, 3H) ppm. ^{13}C NMR (125 MHz, DMSO-d_6): δ = 198.2, 168.4, 158.0, 142.8, 142.7, 140.6, 136.5, 135.8, 135.4, 130.1, 129.8, 128.6, 128.0, 127.8, 124.6, 122.4, 121.0, 120.9, 117.2, 116.2, 115.1, 110.0, 61.1, 52.7, 28.6 ppm. HRMS (ESI): *m/z* calcd. for $C_{27}H_{22}N_4O_3$ $[M+H]^+$ 451.1770; found 451.1778.

4.4.13 (*E*)-5-Benzoyl-3-(3-((1-benzyl-1*H*-1,2,3-triazol-4-yl)methoxy)benzylidene)indolin-2-one (*E*-8j)

Yellow solid; yield: 63%; mp 196-198 °C. IR (KBr): 3401, 3136, 1704, 1613, 1220, 713 cm^{-1}. ^{1}H NMR (500 MHz, DMSO-d_6): δ = 11.10 (s, 1H), 8.37-8.25 (m, 1H), 8.07-7.98 (m, 1H), 7.79-7.47 (m, 6H), 7.42-7.25 (m, 8H), 7.23-6.79 (m, 3H), 5.62 (s, 2H), 5.19 (s, 2H) ppm. ^{13}C NMR (125 MHz, DMSO-d_6): δ = 194.2, 168.8, 158.0, 146.8, 142.8, 142.7, 137.5, 137.2, 135.8, 135.4, 135.2, 132.9, 131.8, 128.9, 128.6, 128.3, 128.0, 127.8, 124.6, 122.4, 121.5,

121.0, 120.6, 116.5, 115.1, 109.9, 61.1, 52.7 ppm. HRMS (ESI): *m/z* calcd. for $C_{32}H_{24}N_4O_3$ $[M+H]^+$ 513.1927; found 513.1927

4.4.14 (*Z*)-3-(3-((1-Benzyl-1*H*-1,2,3-triazol-4-yl)methoxy)benzylidene)-5-(4-methoxybenzyl) indolin-2-one (*Z*-8k)

Yellow solid; yield: 32%; mp 198-200 °C. IR (KBr): 3415, 3029, 1704, 1510, 1478, 1244, 1032, 691 cm^{-1}. ^1H NMR (500 MHz, DMSO-d_6): δ = 10.54 (s, 1H), 8.33 (s, 1H), 8.30 (s, 1H), 7.85 (d, *J* = 7.7 Hz, 1H), 7.73 (s, 1H), 7.58 (s, 1H), 7.39-7.29 (m, 6H), 7.17 (d, *J* = 8.6 Hz, 2H), 7.12 (dd, *J* = 2.2, 8.2 Hz, 1H), 7.06 (d, *J* = 7.9 Hz, 1H), 6.86 (d, *J* = 8.6 Hz, 2H), 6.75 (d, *J* = 7.7 Hz, 1H), 5.61 (s, 2H), 5.18 (s, 2H), 3.84 (s, 2H), 3.70 (s, 3H) ppm. ^{13}C NMR (125 MHz, DMSO-d_6): δ = 167.0, 157.5, 157.4, 142.7, 138.8, 136.3, 135.8, 135.1, 134.4, 133.5, 129.3, 129.1, 128.6, 128.0, 127.8, 127.0, 125.1, 124.9, 124.6, 120.0, 117.2, 117.0, 113.7, 109.1, 61.0, 54.9, 52.7, 39.7 ppm. HRMS (ESI): *m/z* calcd. for $C_{33}H_{28}N_4O_3$ $[M+H]^+$ 529.2240; found 529.2238

4.4.15 (*E*)-3-(3-((1-Benzyl-1*H*-1,2,3-triazol-4-yl)methoxy)benzylidene)-5-(4-methoxybenzyl) indolin-2-one (*E*-8k)

Yellow solid; yield: 39%; mp 138-140 °C. IR (KBr): 3385, 2901, 1703, 1588, 1461, 1221, 1054, 713 cm^{-1}. ^1H NMR (500 MHz, DMSO-d_6): δ = 10.52 (s, 1H), 8.29 (s, 1H), 7.54 (s, 1H), 7.40-7.29 (m, 8H), 7.22 (d, *J* = 7.4 Hz, 1H), 7.12-7.07 (m, 2H), 7.04 (d, *J* = 8.3 Hz, 2H), 6.80-6.75 (m, 3H), 5.61 (s, 2H), 5.16 (s, 2H), 3.71 (s, 2H), 3.67 (s, 3H) ppm. ^{13}C NMR (125 MHz, DMSO-d_6): δ = 168.6, 158.0, 157.4, 142.7, 140.9, 135.8, 135.6, 135.2, 134.4, 132.9, 130.2, 129.6, 129.4, 128.6, 128.0, 127.8, 124.6, 122.7, 121.5, 120.8, 116.2, 115.1, 113.7, 109.8, 61.3, 54.8, 52.7, 39.7 ppm. HRMS (ESI): *m/z* calcd. for $C_{33}H_{28}N_4O_3$ $[M+H]^+$ 529.2240; found 529.2234

4.4.16 (*Z*)-5-Benzhydryl-3-(3-((1-benzyl-1*H*-1,2,3-triazol-4-yl)methoxy)benzylidene) indolin-2-one (*Z*-8l)

Yellow solid; yield: 38%; mp 245-247 °C. IR (KBr): 3392, 2901, 1685, 1578, 1223, 1052, 785 cm^{-1}. ^1H NMR (500 MHz, DMSO-d_6): δ = 10.60 (s, 1H), 8.29 (s, 2H), 7.83 (d, J = 7.7 Hz, 1H), 7.68 (s, 1H), 7.57 (s, 1H), 7.39-7.28 (m, 11H), 7.25-7.19 (m, 2H), 7.18-7.13 (m, 3H), 7.11 (dd, J = 2.2, 8.2 Hz, 1H), 6.93 (d, J = 7.9 Hz, 1H), 6.78 (d, J = 7.9 Hz, 1H), 5.61 (s, 2H), 5.59 (s, 1H), 5.17 (s, 2H) ppm. ^{13}C NMR (125 MHz, DMSO-d_6): δ = 168.6, 157.9, 143.6, 142.6, 141.1, 136.5, 135.8, 135.4, 135.3, 130.9, 129.5, 128.9, 128.7, 128.6, 128.2, 128.0, 127.8, 127.7, 126.0, 124.5, 123.2, 121.0, 120.7, 116.2, 115.0, 109.8, 61.0, 55.2, 52.7 ppm. HRMS (ESI): *m/z* calcd. for $C_{38}H_{30}N_4O_2$ $[M+H]^+$ 575.2447; found 575.2440

4.4.17 (*E*)-5-Benzhydryl-3-(3-((1-benzyl-1*H*-1,2,3-triazol-4-yl)methoxy)benzylidene) indolin-2-one (*E*-8l)

Yellow solid; yield: 35%; mp 220-222 °C. IR (KBr): 3380, 3136, 2921, 1685, 1578, 1446, 1223, 1012, 785 cm^{-1}. ^1H NMR (500 MHz, DMSO-d_6): δ = 10.57 (s, 1H), 8.22 (s, 1H), 7.52 (s, 1H), 7.39-7.28 (m, 8H), 7.26-7.19 (m, 4H), 7.18-7.11 (m, 3H), 7.09-6.99 (m, 6H), 6.83 (d, J = 8.0 Hz, 1H), 5.60 (s, 2H), 5.47 (s, 1H), 5.07 (s, 2H) ppm. ^{13}C NMR (125 MHz, DMSO-d_6): δ = 168.6, 157.9, 143.7, 142.6, 141.1, 136.5, 135.9, 135.4, 135.4, 130.9, 129.6, 128.9, 128.7, 128.6, 128.2, 128.0, 127.8, 127.7, 126.0, 124.5, 123.2, 121.0, 116.2, 115.0, 109.8, 61.0, 55.2, 52.7 ppm. HRMS (ESI): *m/z* calcd. for $C_{38}H_{30}N_4O_2$ $[M+H]^+$ 575.2447; found 575.2440

4.4.18 (*Z*)-3-(3-((1-Benzyl-1*H*-1,2,3-triazol-4-yl)methoxy)benzylidene)-5-(3-phenyl-1-(p-tolyl)prop-2-yn-1-yl)indolin-2-one (*Z*-8m)

Yellow solid; yield: 33%; mp 202-204 °C. IR (KBr): 3324, 3137, 1704, 1690, 1588, 1462, 1220, 1028, 740 cm^{-1}. ^1H NMR (500 MHz, DMSO-d_6): δ = 10.63 (s, 1H), 8.32 (s, 1H), 8.30 (s, 1H), 7.84 (d, J = 7.7 Hz, 1H), 7.78-7.75 (m, 1H), 7.52-7.49 (m, 1H), 7.40-7.27 (m, 12H),

7.26 (dd, *J* = 2.7, 8.0 Hz, 1H), 7.17 (d, *J* = 7.9 Hz, 2H), 7.13 (dd, *J* = 2.2, 8.0 Hz, 1H), 7.08 (d, *J* = 7.7 Hz, 1H), 6.82 (d, *J* = 7.9 Hz, 1H), 5.61 (s, 2H), 5.32 (s, 1H), 5.18 (s, 2H), 2.26 (s, 3H) ppm. ^{13}C NMR (125 MHz, DMSO-d_6): δ = 167.0, 157.5, 142.8, 139.5, 139.0, 135.9, 135.8, 135.0, 135.0, 131.3, 131.2, 129.1, 129.1, 128.6, 128.5, 128.4, 128.3, 128.0, 127.8, 127.2, 127.1, 126.8, 125.2, 125.0, 124.6, 122.6, 119.0, 109.4, 91.0, 84.0, 61.0, 52.7, 41.9, 20.5 ppm. HRMS (ESI): *m/z* calcd. for $C_{41}H_{32}N_4O_2$ $[M+H]^+$ 613.2604; found 613.2604

4.4.19 (*E*)-3-(3-((1-Benzyl-1*H*-1,2,3-triazol-4-yl)methoxy)benzylidene)-5-(3-phenyl-1-(p-tolyl)prop-2-yn-1-yl)indolin-2-one (*E*-8m)

Yellow solid; yield: 45%; mp 183-185 °C. IR (KBr): 3358, 2901, 1702, 1605, 1445, 1253, 1048, 691 cm^{-1}. ^{1}H NMR (300 MHz, DMSO-d_6): δ = 10.59 (s, 1H), 8.23 (s, 1H), 7.77 (m, 1H), 7.57 (s, 1H), 7.40-7.26 (m, 13H), 7.26-7.21 (m, 3H), 7.09 (d, *J* = 7.9 Hz, 1H), 7.05-7.02 (m, 2H), 6.85 (d, *J* = 8.0 Hz, 1H), 5.59 (s, 2H), 5.25 (s, 1H), 5.13 (s, 2H), 2.21 (s, 3H) ppm. ^{13}C NMR (75 MHz, DMSO-d_6): δ = 168.5, 158.0, 142.6, 141.6, 138.9, 135.8, 135.6, 135.5, 134.8, 131.1, 129.5, 129.3, 129.1, 128.6, 128.4, 128.2, 128.0, 127.8, 127.6, 127.1, 124.5, 122.4, 121.5, 121.4, 121.0, 116.2, 115.1, 109.9, 90.7, 84.0, 61.1, 52.7, 41.4, 20.4 ppm. HRMS (ESI): *m/z* calcd. for $C_{41}H_{32}N_4O_2$ $[M+H]^+$ 613.2604; found 613.2602

4.5 Pharmacology

4.5.1 Cell culture

Cells were obtained from National Centre for Cell Science (NCCS) Pune, India and stocks were maintained in the laboratory. Breast (BT549 and MDA-MB-231), prostate (PC-3 and DU145), lung (A549) and cervical (HeLa) cancer cells were grown in tissue culture flasks in DMEM (Dulbecco modified Eagle medium, Sigma) or RPMI (Roswell Park Memorial Institute medium) supplemented with 10% fetal bovine serum with 1X stabilized antibiotic-

antimycotic solution (Sigma) in a CO_2 incubator at 37 ^oC with 5% CO_2 and 90% relative humidity.

4.5.2 MTT assay

The anticancer activity of all newly synthesized compounds was determined using MTT assay. 3-5x10^3 cells per well were seeded in 100 µL DMEM or RPMI, supplemented with 10% FBS in each well of 96-well microculture plates and incubated for 48 h at 37 °C in a CO_2 incubator. Compounds, diluted to the desired concentrations in culture medium, were added to the wells with respective vehicle control. After 48 h of incubation, drugs containing media was removed and 100 µL MTT (3-(4,5-dimethylthiazol-2-yl)-2,5-diphenyl tetrazolium bromide) (0.5mg/mL) was added to each well and the plates were further incubated for 4 h. Then, the supernatant from each well was carefully removed, formazon crystals were dissolved in 200 µL of DMSO and absorbance was recorded at 570 nm wavelength.

4.5.3 Acridine orange–ethidium bromide (AO–EB) staining

DU145 cells were plated at a concentration of 1×10^6 cell/ml and treated with different concentration of compound ***Z*-8l**. Plates were incubated in an atmosphere of 5% CO_2 at 37 °C for 48 h. 10 µL of fluorescent dyes containing Acridine Orange (AO) and Ethidium Bromide (EB) added into each well in equal volumes (10 μg/mL) respectively and within 10 min the cells were visualized under fluorescence microscope (Nikon, Inc. Japan) with excitation (488 nm) and emission (550 nm) at 200x magnification.

4.5.4 DAPI Nucleic Acid Staining

Nuclear morphological changes were observed through DAPI staining. After treatment with ***Z*-8l** for 48 h in DU145 cells, cells were washed with PBS and permeabilized with 0.1 % Tween 20 for 10 min followed by staining with 1 µM DAPI. Control and Treated cells were

observed with fluorescence microscope (Model: Nikon, Japan) with excitation at 359 nm and emission at 461 nm using DAPI filter at 200X magnification.

4.5.5 Cell cycle analysis

Flow cytometric analysis (FACS) was performed to calculate the distribution of the cell population through the cell cycle phases. DU145 cancer cells were incubated with compound ***Z*-8l** at varied concentration of 2.5 µM, and 5.0 µM for 24 h. Untreated and treated cells were harvested, washed with PBS, fixed in ice-cold 70% ethanol and stained with propidium iodide (50 µg/mL, sigma aldrich) in the presence of RNase A (20 µg/mL) containing 0.1% Triton X-100 for 30 min at 37 ^{o}C in dark, and about 10000 events were analyzed by flow cytometer (BD FACSVerse^{TM}, USA).

4.5.6 Annexin V binding assay

DU145 cells ($1x10^{6}$) were seeded in six-well plates and allowed to grow overnight. The medium was then replaced with complete medium containing compound ***Z*-8l** at 1.25, 2.5 and 5.0 µM concentrations. After 24 h of treatment, cells from the supernatant and adherent monolayer cells were harvested by trypsinization, washed with PBS at 3000 rpm. Then the cells were processed with Annexin V-assay kit (FITC Annexin V Apoptosis Detection Kit, BD Pharmingen^{TM}) according to the manufacturer's instruction. Further, flow cytometric analysis was performed using a flow cytometer (BD FACSVerse^{TM}, USA).

4.5.7 Measurement of reactive oxygen species (ROS) levels

DU145 cells were plated in 6 well plates at a density of 1×10^{6} cells/mL and allowed to adhere for overnight. The cells were treated with 1.25, 2.5 and 5 µM concentrations of the compound ***Z*-8l** for 24 h. The medium was replaced with culture medium containing DCFDA dye (10 µM) and further incubated for 30 min at room temperature in dark. The fluorescence intensity

from each sample was analysed by spectrofluorometer at an excitation and emission wavelength of 488 and 525 nm, respectively.

4.5.8 Measurement of Mitochondrial Membrane Potential

DU145 cells (1×10^6 cells/mL) were seeded in 6 well plates and allowed to adhere for overnight. The cells were incubated with 1.25, 2.5 and 5 µM concentrations of the compound ***Z*-8l** for 24 h. Cells were collected, washed with PBS and resuspended in solution of JC-1 (2.5 µg/mL) and incubated for 45 min in incubator at 37 °C . The cells were washed twice with PBS and cells were trypsinized, centrifuged and analysed by flow cytometer (BD FACSVerse™, USA).

4.5.9 Western blotting analysis

Primary antibodies against Bax, Bcl-2, PARP, Cyt c, β-actin and HRP conjugated antirabbit secondary antibodies were purchased from Cell Signaling Technology (Beverly, MA, USA). Equal amounts of protein sample (25 µg/lane) from each experimental group and were separated by SDS–polyacrylamide gel electrophoresis. Then the protein bands were transferred to polyvinylidene fluoride membrane (Pierce Biotechnology, Rockford, IL, USA) for western blotting. Membranes were blocked with 3% bovine serum albumin in TBS buffer (pH-7.4) and incubated with the indicated antibodies overnight at 4 °C. β-actin (1:1000) was used for equal loading. After washing the membranes in TBST buffer, membranes were exposed to the HRP-conjugated secondary antibodies (1:5000) for 2 h at room temperature. The reactive bands were visualized with chemiluminescent detection reagents (Supersignal West Pico, Pierce Biotechnology, Rockford, IL, USA). The densitometry analysis of the blots was performed by using Image J software, NIH, USA.

Acknowledgements

Authors are thankful to DoP, Ministry of Chemicals & Fertilizers, Govt. of India, New Delhi, for the award of NIPER fellowship.

References

1. K.R. Senwar, T. Srinivasa Reddy, D. Thummuri, P. Sharma, V.G.M. Naidu, G. Srinivasulu, N. Shankaraiah, Eur. J. Med. Chem. 118 (2016) 34–46.
2. R.L. Siegel, K.D. Miller, A. Jemal, CA Cancer J. Clin. 65 (2015) 5–29.
3. (a) A. Millemaggi, R.J.K. Taylor, Eur. J. Org. Chem. 24 (2010) 4527–4547; (b) S. Peddibhotla, Curr. Bioact. Compd. 5 (2009) 20–38; (c) G.S. Singh, Z.Y. Desta, Chem. Rev. 112 (2012) 6104–6155; (d) C.V. Galliford, K.A. Scheidt, Angew. Chem. Int. Ed. 46 (2007) 8748–8758.
4. G.H. Zheng, J.J. Shen, Y.C. Zhan, H. Yi, S.T. Xue, Z. Wang, X.Y. Ji, R. Li, Eur. J. Med. Chem. 81 (2014) 277–288.
5. G. Bhaskar, Y. Arun, C. Balachandran, C. Saikumar, P.T. Perumal, Eur. J. Med. Chem. 51 (2012) 79–91.
6. Y. Kia, H. Osman, R.S. Kumar, V. Murugaiyah, A. Basiri, S. Perumal, H.A. Wahab, C.S. Bing, Biorg. Med. Chem. 21 (2013) 1696–1707.
7. K. Huber, J. Schemies, U. Uciechowska, J.M. Wagner, T. Rumpf, F. Lewrick, R. Süss, W. Sippl, M. Jung, F. Bracher, J. Med. Chem. 53 (2010) 1383–1386.
8. A. Leoni, A. Locatelli, R. Morigi, M. Rambaldi, Expert Opin. Ther. Pat. 26 (2016) 149–173.
9. C.R. Prakash, S. Raja, Mini. Rev. Med. Chem. 12 (2012) 98–119.
10. G. J. Roth, R. Binder, F. Colbatzky, C. Dallinger, R. Schlenker-Herceg, F. Hilberg, S.L. Wollin, R. Kaiser, J. Med. Chem. 2015, 58, 1053–1063.

11. R.J. Motzer, M.D. Michaelson, B.G. Redman, G.R. Hudes, G. Wilding, R.A. Figlin, M.S. Ginsberg, S.T. Kim, C.M. Baum, S.E. DePrimo, J.Z. Li, C.L. Bello, C.P. Theuer, D.J. George, B.I. Rini, J. Clin. Oncol. 24 (2006) 16–24.
12. H. Prenen, J. Cools, N. Mentens, C. Folens, R. Sciot, P. Schöffski, A.V. Oosterom, P. Marynen, M. Debiec-Rychter, Clin. Cancer Res. 12 (2006) 2622–2627.
13. X. Chen, T. Yang, A. Deivasigamani, M.K. Shanmugam, K.–M. Hui, G. Sethi, M.–L. Go, ChemMedChem 10 (2015) 1548–1558.
14. A.F. Watson, J. Liu, K. Bennaceur, C.J. Drummond, J.A. Endicott, B.T. Golding, R.J. Griffin, K. Haggerty, X. Lu, J.M. McDonnell, D.R. Newell, M.E.M. Noble, C.H. Revill, C. Riedinger, Q. Xu, Y. Zhao, J. Lunec, I.R. Hardcastle, Bioorg. Med. Chem. Lett. 21 (2011) 5916–5919.
15. W. Zhang, M.-L. Go, Bioorg. Med. Chem. 17 (2009) 2077–2090.
16. R. Kumar, J. Arora, A.K. Prasad, N. Islam, A.K. Verma, Med. Chem. Res. 22 (2013) 5624–5631.
17. M. Aufort, J. Herscovici, P. Bouhours, N. Moreau, C. Girard, Bioorg. Med. Chem. Lett. 18 (2008) 1195–1198.
18. R. Alvarez, S. Velázquez, A. San-Félix, S. Aquaro, E. De Clercq, C.F. Perno, A. Karlsson, J. Balzarini, M.J. Camarasa, J. Med. Chem. 37 (1994) 4185–4194.
19. M.J. Genin, D.A. Allwine, D.J. Anderson, M.R. Barbachyn, D.M. Emmert, S.A. Garmon, D.R. Graber, K.C. Grega, J.B. Hester, D.K. Hutchinson, J. Morris, R.J. Reischer, C.W. Ford, G.E. Zurenko, J.C. Hamel, R.D. Schaadt, D. Stapert, B.H. Yagi, J. Med. Chem. 43 (2000) 953–970.
20. L.L. Brockunier, E.R. Parmee, H.O. Ok, M.R. Candelore, M.A. Cascieri, L.F. Colwell, L. Deng, W.P. Feeney, M.J. Forrest, G.J. Hom, D.E. MacIntyre, L. Tota, M.J. Wyvratt, M.H. Fisher, A.E. Weber, Bioorg. Med. Chem. 10 (2000) 2111–2114.

21. V. Pande, M.J. Ramos, Bioorg. Med. Chem. Lett. 15 (2005) 5129–5135.

22. A. Krasinski, Z. Radic, R. Manetsch, J. Raushel, P. Taylor, B.K. Sharpless, H.C. Kolb, J. Am. Chem. Soc. 127 (2005) 6686–6692.

23. A. Nagarsenkar, S.K. Prajapti, S.D. Guggilapu, S. Birineni, S.S. Kotapalli, R. Ummanni, B.N. Babu, Med. Chem. Commun. 7 (2016) 646–653.

24. P. Singh, M. Kaur, W. Holzer, Eur. J. Med. Chem. 45 (2010) 4968–4982.

25. R. Goel, V. Luxami, K. Paul, RSC Adv. 5 (2015) 37887–37895.

26. L.S. Campbell-Verduyn, L. Mirfeizi, R.A. Dierckx, P.H. Elsinga, B.L. Feringa, Chem. Comm. (2009) 2139–2141.

27. L.S. Campbell-Verduyn, L. Mirfeizi, R.A. Dierckx, P.H. Elsinga, B.L. Feringa, Bioorg. Med. Chem. Lett. 23 (2013) 5523–5527.

28. Z.-X. Wang, Z.-G. Zhao, J. Heterocyclic Chem. 44 (2007) 89–92.

29. R. Venkataramanarao, V.V. Sureshbabu, *Synlett* **2007**, 2492–2496.

30. L. Sun, N. Tran, F. Tang, H. App, P. Hirth, G. McMahon, C. Tang, J. Med. Chem. 41 (1998) 2588–2603.

31. S. Shrivastava, P. Kulkarni, D. Thummuri, M.K. Jeengar, V.G.M. Naidu, M. Alvala, G.B. Reddy, S. Ramakrishna, Apoptosis 19 (2014) 1148–1164.

32. U.V. Mallavadhani, N.R. Vanga, M.K. Jeengar, V.G.M. Naidu, Eur. J. Med. Chem. 74 (2014) 398–404.

33. S.G. Kennedy, E.S. Kandel, T.K. Cross, N. Hay, Mol. Cell Biol. **19 (**1999) 5800–5810.

34. S.K. Prajapti, A. Nagarsenkar, S.D. Guggilapu, K.K. Gupta, L. Allakonda, M.K. Jeengar, V.G.M. Naidu, B.N. Babu, Bioorg. Med. Chem. Lett. 26 (2016) 3024–3028.

35. L.J. Browne, C. Gude, H. Rodriguez, R.E. Steele, A. Bhatnager, J. Med. Chem. 34 (1991) 725–736.

36. T.S. Reddy, H. Kulhari, V.G. Reddy, V. Bansal, A. Kamal, R. Shukla, Eur. J. Med. Chem. 101 (2015) 790–805.

37. P. Sharma, K.R. Senwar, M.K. Jeengar, T.S. Reddy, V.G.M. Naidu, A. Kamal and N. Shankaraiah, Eur. J. Med. Chem. 104 (2015) 11.

38. (a) M.A. O'Brien, R.A. Moravec, T.L. Riss, BioTechniques 30 (2001) 886–891; (b) X. Lu, C. Li, Y.-K. Wang, K. Jiang, X.-D. Gai, Oncol. Lett. 7 (2014) 1992–1996.

Figures captions, Tables, Figures and Schemes

Figure 1. Structure of some representative bioactive compounds containing oxindole (a, b, c) and triazole (d, e, f) moieties.

Figure 2. Design of novel triazole linked 3-benzylidene isatin hybrids as anticancer agents.

Figure 3. Schematic representation of characteristic NOEs of compound ***Z*-8a**.

Figure 4. Expanded ROESY spectrum of compound ***Z*-8a** in DMSO-d_6 (500 MHz, 27 °C) showing characteristic NOEs.

Figure 5. AO/EB staining of compound ***Z*-8l** in DU145 cells. Apoptotic features such as membrane blebbing, apoptotic body formations and dead cells were clearly observed in treated cells with indicated conc. of ***Z*-8l** in conc. dependent manner.

Figure 6. Assessment of nuclear morphological changes by DAPI staining in DU145 cells after 48 h. ***Z*-8l** treated DU145 cells have displayed nuclear apoptotic characteristics such as nuclear fragmentation and shrunken nuclei

Figure 7. Effect of compound ***Z*-8l** on cell cycle progression of DU145 cells. The analysis of cell cycle distribution was performed by using propidium iodide staining method. Data represent one of three independent experiments.

Figure 8. Flow cytometry analysis of apoptotic cells after Annexin V-FITC/propidium iodide (PI) staining (representative result of three independent experiments).

Figure 9. Effect of compound ***Z*-8l** on intracellular Reactive Oxygen Species levels. DU145 cells were treated with different concentrations of the compound ***Z*-8l** and stained with DCFDA .and fluorescence readings were determined in spectrophotometer. *P < 0.05, **P < 0.01, ***P < 0.001 Vs NC. And ^P< 0.05, ^^P< 0.01, ^^^P<0.001 Vs respective drug

treatment. Statistical analyses were performed using one-way analysis of variance, followed by the bonferroni multiple comparison test.

Figure 10. Effect of compound ***Z*-8l** on mitochondrial membrane potential (DΨm). DU145 cells were treated with different concentrations (1.25, 2.5 and 5.0 µM respectively) of compound ***Z*-8l** and incubated with JC-1 and analysed by flow cytometer (BD FACSVerse™, USA).

Figure 11. Effect of ***Z*-8l** on various protein expressions in DU145 cell line: Results were expressed as mean ± SEM (n=6). NC: Normal control, 1 & 3 µM ***Z*-8l** indicate cells treated with 1 & 3 µM of ***Z*-8l** and 5 µM **S** (sunitinib) indicate cells treated with 5 µM of sunitinib for 48 h. *P < 0.05, **P < 0.01, ***P < 0.001 Vs NC. Statistical analyses were performed using one-way analysis of variance, followed by the two-tailed Student's t-test.

Table 1. *In vitro* anticancer activity of compounds **[*E*-8(a-b, d, f-m)** and ***Z*-8(a-c, e, i, k-m)]**.

Compound	IC_{50} (µM)						
	DU145 [a]	**PC-3** [b]	**MDA-MB-231** [c]	**BT549** [d]	**A549** [e]	**HeLa** [f]	**RWPE-1** [g]
***Z*-8a**	ND	34.45 ± 0.36	ND	>50	31.5±0.95	ND	-
***E*-8a**	31.7±0.7	29.51 ± 0.78	ND	>50	>50	32.33 ± 0.44	-
***Z*-8b**	ND	31.67 ± 1.02	>50	>50	43.3±7.1	33.8 ± 0.6	-
***E*-8b**	25.6±4.2	37.13 ± 1.15	**11.7±0.56**	ND	26.7±0.77	22.01 ± 4.18	-
***Z*-8c**	24.2±0.12	>50	ND	ND	>50	ND	-
***E*-8d**	20.1±1.61	>50	>50	>50	>50	>50	-
***Z*-8e**	35.1±0.79	>50	>50	>50	>50	>50	-
***E*-8f**	**5.7±0.4**	>50	ND	>50	**9.6±0.38**	ND	-
***E*-8g**	ND	>50	>50	>50	>50	>50	-
***E*-8h**	ND	>50	>50	>50	>50	>50	-
***Z*-8i**	>50	>50	>50	>50	36.3±3.07	>50	-
***E*-8i**	>50	>50	>50	>50	>50	>50	-
***E*-8j**	>50	>50	>50	>50	>50	>50	-
***Z*-8k**	**6.7±0.35**	>50	20.4±1.76	36.0±0.89	30.5±0.78	**7.7 ± 1.2**	-
***E*-8k**	>50	32.2 ± 0.5	>50	>50	>50	ND	-
***Z*-8l**	**3.7±0.05**	**17.2 ± 1.6**	ND	**15.8±0.67**	**14.7±0.38**	**4.28 ± 0.16**	21.4±0.74
***E*-8l**	>50	>50	>50	>50	>50	>50	-
***Z*-8m**	>50	>50	>50	>50	>50	>50	-
***E*-8m**	28.9±1.09	>50	ND	>50	36.6±1.36	32.8 ± 0.5	-
6a	>50	>50	>50	>50	>50	>50	-
S	16.3±0.5	12.6±1.0	7.4±0.5	15.5±0.5	14.4±0.3	10.4±0.45	25.2±1.4

[a, b]: Human prostate cancer cell line; [c, d]: Human breast cancer cell line; [e]: Human lung cancer cell line; [f]: Human cervical cancer cell line; [g]: Normal prostate cancer cell line; ND: Not determined; S: Sunitinib

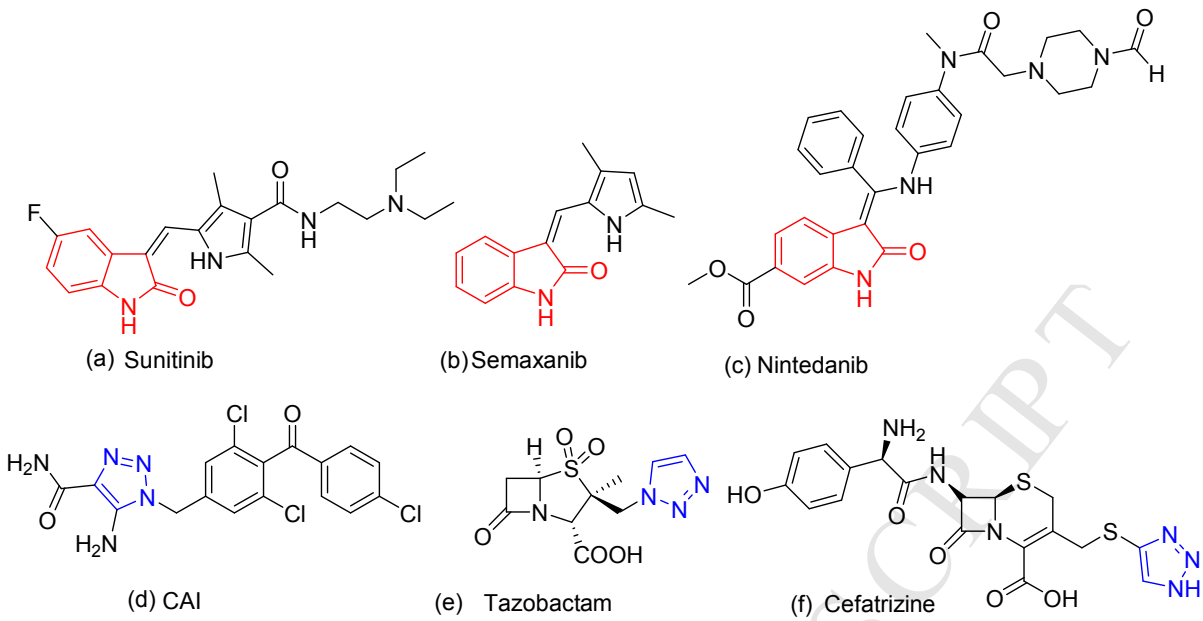

Figure 1. Structure of some representative bioactive compounds containing oxindole (a, b, c) and triazole (d, e, f) moieties.

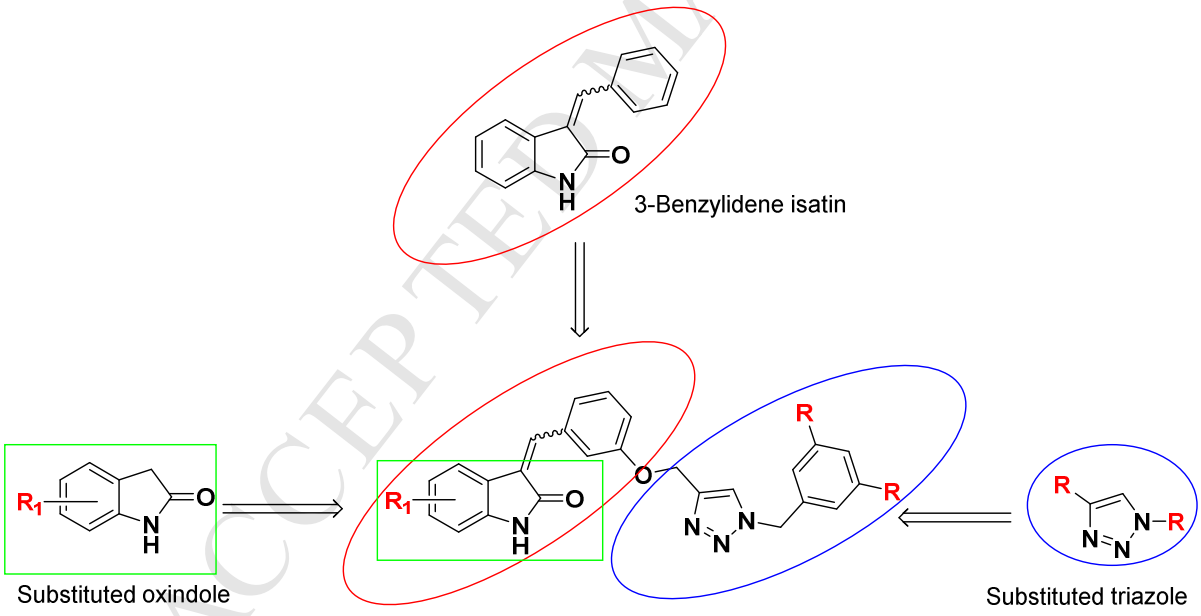

Figure 2. Design of novel triazole linked 3-benzylidene isatin hybrids as anticancer agents.

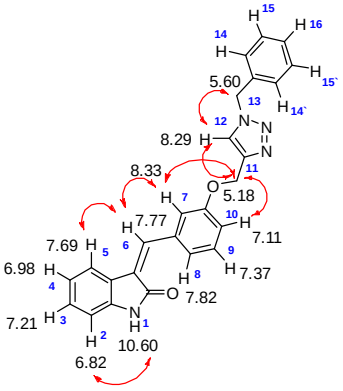

Figure 3. Schematic representation of characteristic NOEs of compound ***Z*-8a**.

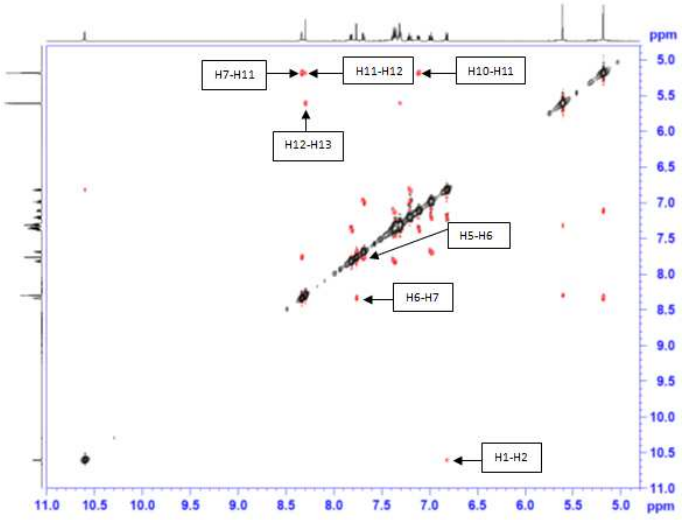

Figure 4. Expanded ROESY spectrum of compound ***Z*-8a** in DMSO-d_6 (500 MHz, 27 °C) showing characteristic NOEs.

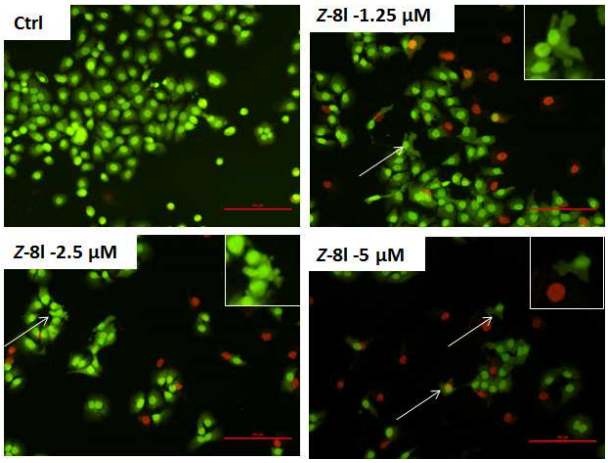

Figure 5. AO/EB staining of compound ***Z*-8l** in DU145 cells. Apoptotic features such as membrane blebbing, apoptotic body formations and dead cells were clearly observed in treated cells with indicated conc. of ***Z*-8l** in conc. dependent manner.

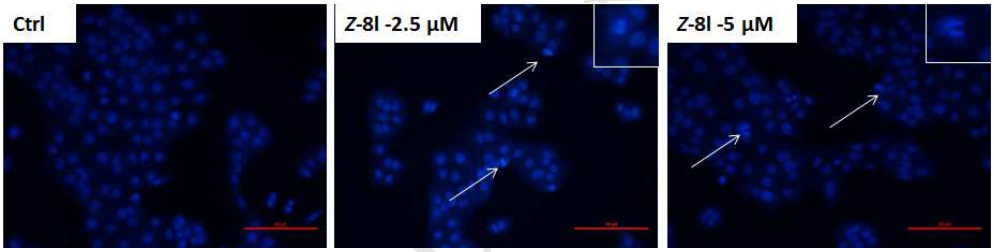

Figure 6. Assessment of nuclear morphological changes by DAPI staining in DU145 cells after 48 h. ***Z*-8l** treated DU145 cells have displayed nuclear apoptotic characteristics such as nuclear fragmentation and shrunken nuclei

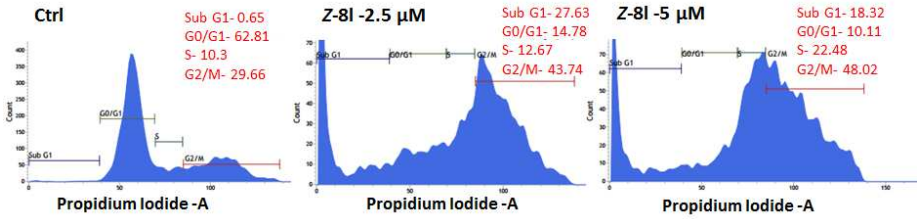

Figure 7. Effect of compound ***Z*-8l** on cell cycle progression of DU145 cells. The analysis of cell cycle distribution was performed by using propidium iodide staining method. Data represent one of three independent experiments.

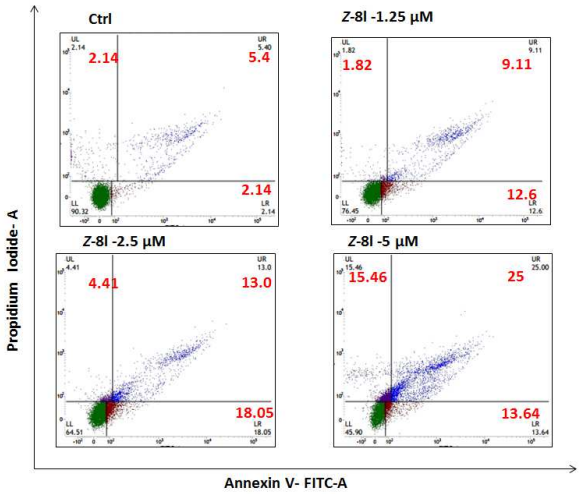

Figure 8. Flow cytometry analysis of apoptotic cells after Annexin V-FITC/propidium iodide (PI) staining (representative result of three independent experiments).

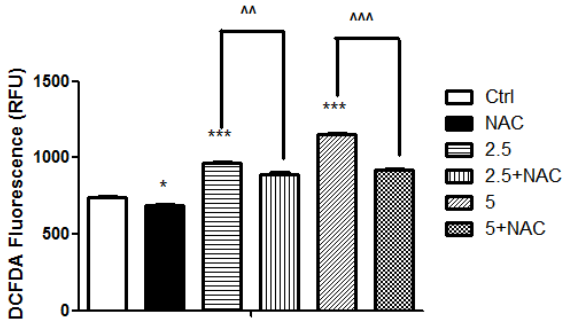

Figure 9. Effect of compound ***Z*-8l** on intracellular Reactive Oxygen Species levels. DU145 cells were treated with different concentrations of the compound ***Z*-8l** and stained with DCFDA .and fluorescence readings were determined in spectrophotometer. *P < 0.05, **P < 0.01, ***P < 0.001 Vs NC. And ^P< 0.05, ^^P< 0.01, ^^^P<0.001 Vs respective drug treatment. Statistical analyses were performed using one-way analysis of variance, followed by the bonferroni multiple comparison test.

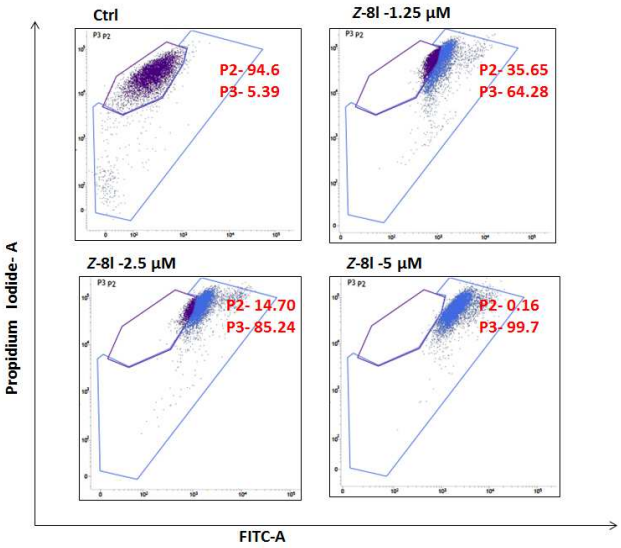

Figure 10. Effect of compound ***Z*-8l** on mitochondrial membrane potential (DΨm). DU145 cells were treated with different concentrations (1.25, 2.5 and 5.0 µM respectively) of compound ***Z*-8l** and incubated with JC-1 and analysed by flow cytometer (BD FACSVerse™, USA).

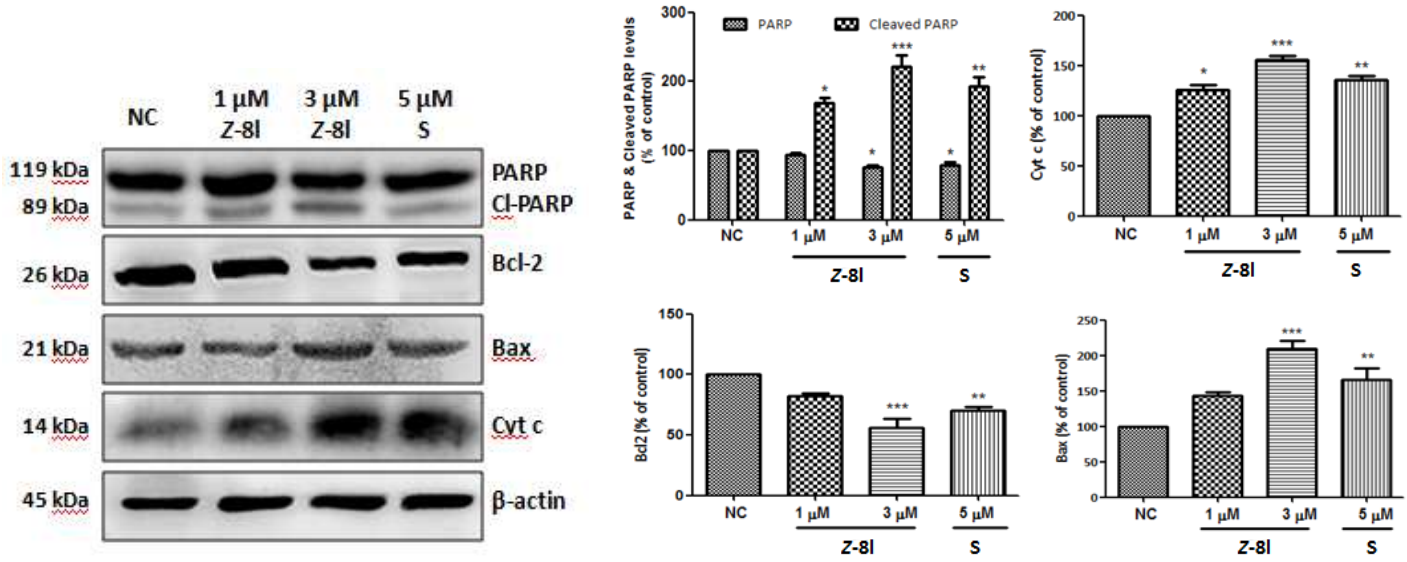

Figure 11. Effect of ***Z*-8l** on various protein expressions in DU145 cell line: Results were expressed as mean ± SEM (n=6). NC: Normal control, 1 & 3 µM ***Z*-8l** indicate cells treated with 1 & 3 µM of ***Z*-8l** and 5 µM S (sunitinib) indicate cells treated with 5 µM of sunitinib for 48 h. *P < 0.05, **P < 0.01, ***P < 0.001 Vs NC. Statistical analyses were performed using one-way analysis of variance, followed by the two-tailed Student's t-test.

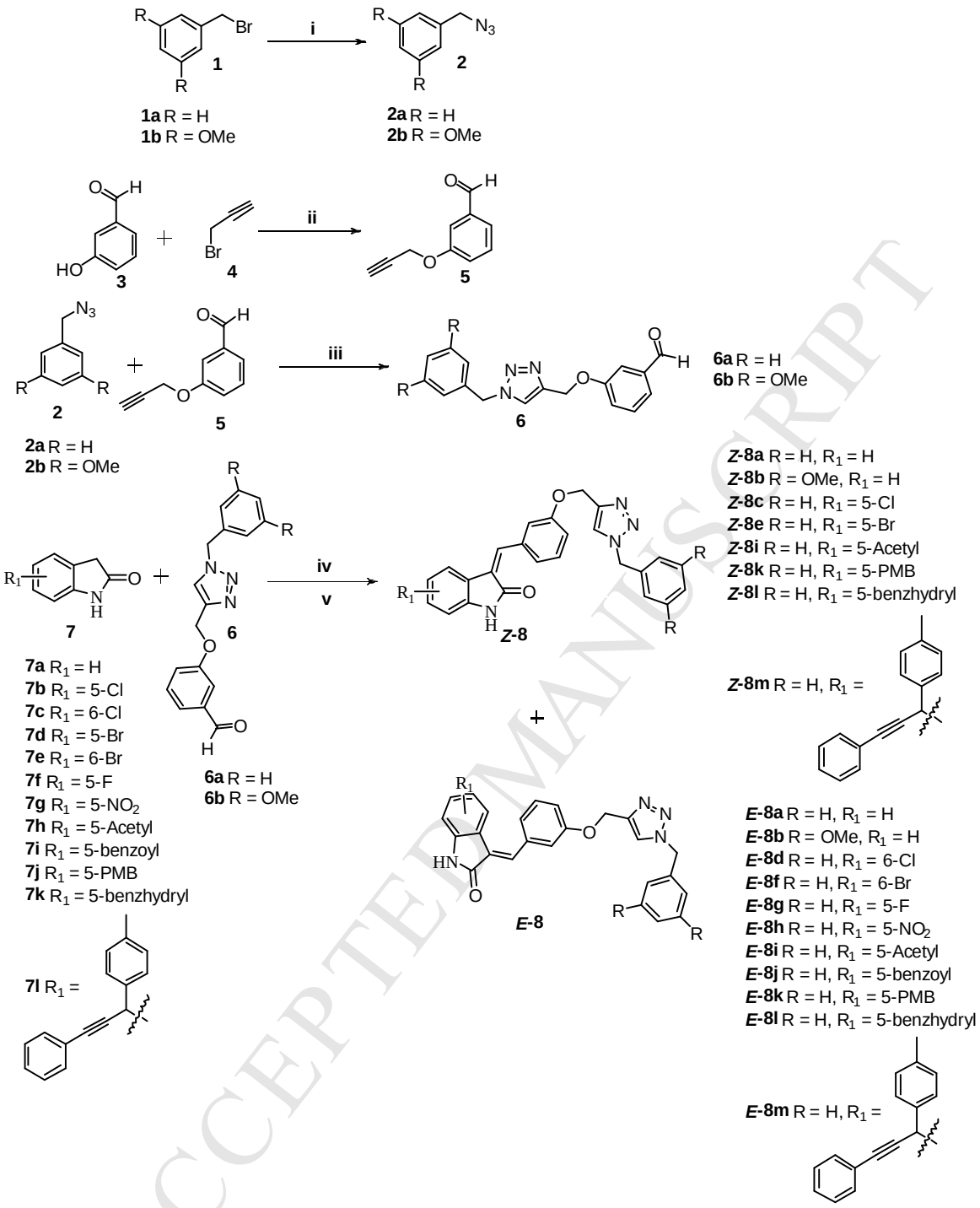

Scheme 1. Synthesis of 3-(3-((1-phenyl-1*H*-1,2,3-triazol-4-yl)methoxy)benzylidene)indolin-2-one derivatives; Reagents and conditions: (i) NaN_3, acetone/water (1:1), rt, 12 h; (ii) K_2CO_3, acetonitrile, reflux, 6 h; (iii) CuI, *t*-butanol/water (1:1), 40 °C, 48 h; (iv) piperidine, ethanol, reflux, 3-4 h; (v) isomers separated by using column chromatography.

Research Highlights

- ✓ Novel triazole linked benzylidene-isatins were synthesized.
- ✓ Cytotoxicity study on DU145 (prostate), PC-3 (prostate), MDA-MB-231 (breast), BT549 (breast), A549 (lung) and HeLa (cervical) human cancer cell lines and one normal cell line (RWPE-1).
- ✓ Compound *Z*-**8l** induced apoptosis, increased the level of superoxide ROS, caused the collapse of DΨm and G2/M cell cycle arrest.
- ✓ *Z*-**8l** activated Cyt-C, cleaved PARP, and caused changes in expression of Bax and Bcl-2.